Published in final edited form as:
Science. 2020 December 18; 370(6523): . doi:10.1126/science.aaz3136.

Perirhinal input to neocortical layer 1 controls learning

Guy Doron[#1,*], **Jiyun N. Shin**[#1], **Naoya Takahashi**[2], **Moritz Drüke**[1], **Christina Bocklisch**[1], **Salina Skenderi**[1], **Lisa de Mont**[1], **Maria Toumazou**[1], **Julia Ledderose**[1], **Michael Brecht**[3,4], **Richard Naud**[5,6], **Matthew E. Larkum**[1,4,*]

[1]Institute for Biology, Humboldt-Universität zu Berlin, D-10117 Berlin, Germany

[2]University of Bordeaux, CNRS, Interdisciplinary Institute for Neuroscience, IINS, UMR 5297, 33000 Bordeaux, France

[3]Bernstein Center for Computational Neuroscience, Humboldt-Universität zu Berlin, D-10115 Berlin, Germany

[4]NeuroCure Cluster, Charité - Universitätsmedizin Berlin, D-10117 Berlin, Germany

[5]uOttawa Brain and Mind Institute, Department of Cellular and Molecular Medicine, University of Ottawa, Ottawa, Ontario, K1H 8M5, Canada

[6]Department of Physics, University of Ottawa, Ottawa, K1N 6N5, Canada

[#] These authors contributed equally to this work.

Abstract

Hippocampal output influences memory formation in the neocortex but this process is poorly understood because the precise anatomical location and the underlying cellular mechanisms remain elusive. Here, we show that perirhinal input, predominantly to sensory cortical layer 1 (L1), controls hippocampal-dependent associative learning. This process was marked by the emergence of distinct firing responses in defined subpopulations of L5 pyramidal neurons whose tuft dendrites receive perirhinal inputs in L1. Learning correlated with burst firing and enhancement of dendritic excitability and was suppressed by disruption of dendritic activity. Furthermore, bursts, but not regular spike trains, were sufficient to retrieve learned behavior. We conclude that hippocampal information arriving at L5 tuft dendrites in neocortical L1 mediates memory formation in the neocortex.

Hippocampal-cortical dialogue mediates stabilization of memory traces (1, 2). However, the distributed nature of long-term memory representation in the neocortex has challenged research into the underlying mechanisms of this process. In particular, how the medial temporal system modulates primary sensory cortices during learning remains largely unknown. For hippocampal-independent learning paradigms there is converging evidence

[*]Corresponding authors. matthew.larkum@hu-berlin.de, guydoron@gmail.com .

Author contributions: Author contributions G.D., J.N.S. and M.E.L. planned and designed the experiments and wrote the manuscript. G.D., J.N.S., N.T., S.S, L.D., M.D., and C.B. performed the experiments. J.L. and M.T performed the histology. G.D., J.N.S, N.T, R.N. and C.B. analyzed the data. M.E.L., G.D., J.N.S., N.T, C.B., M.B. and R.N. developed data analysis methodologies and consulted on experimental design, reviewed and edited the manuscript. All authors approved the final version of the paper.

Competing Interests: The authors declare no competing interests.

Europe PMC Funders Author Manuscripts

suggesting that neocortical layer 1 (L1) is a locus for plasticity (3–6) involving activity in the distal tuft dendrites of pyramidal neurons that innervate L1 (4, 7–9). We hypothesized that inputs from the medial temporal system also influence neocortical L1 to control memory formation during hippocampal-dependent tasks. We investigated this in the primary somatosensory cortex (S1) of rodents. Application of the tracer, Fast Blue, to L1 of S1, retrogradely labelled presynaptic neurons in the deep layers of the perirhinal cortex (Fig. 1A, bottom left). Conversely, expression of AAV-ChR2-EYFP injected into the deep layers of the perirhinal cortex densely labelled axons in L1 of S1 (Fig. 1A, bottom right), confirming that the perirhinal cortex is the last station in the medial temporal loop projecting to S1 in rodents (Fig. 1A, right and Fig. S1) (2, 10–12).

We used a fast-learning, associative and cortex-dependent task (13). Rodents were trained to report short (200 ms) direct electrical microstimulation (μStim) pulses in layer 5 (L5) of S1 (Fig. 1B) where the μStim detection threshold is lowest (13). During training, animals received a block (5 repetitions) of μStim paired with reward (sweetened water) regardless of their licking responses to the stimulus. Following a brief training period (1-2 blocks of pairings), learning was tested by making the reward available only if the animal actively licked within a response window of 100–1200 ms following μStim onset (‘Hit’, Fig. 1B). Both mice and rats learned this task rapidly within the first session and became experts after a median of 3 sessions (one session/day, see Methods). Ipsilateral injections of lidocaine in the hippocampus prevented learning of the task (Fig. S2). Making behavior contingent on μStim of S1 allowed us to define the area of interest and temporal window. Moreover, it allowed us to precisely target the perirhinal projection to L1 of S1. To confirm the involvement of the perirhinal cortex in learning of μStim and reward association, we measured perirhinal axonal Ca^{2+} activity using two-photon imaging of perirhinal axons in L1 of S1 prior to and following a single session of μStim training (Fig. 1C and Fig. S3). We expressed GCaMP6s in the perirhinal cortex via viral (AAV) injection >3 weeks previously. Perirhinal axons responded only weakly to μStim before its association with reward but were significantly modulated following the first training session. Providing the reward alone (not coupled with μStim) did not evoke such axonal Ca^{2+} activity in perirhinal neurons.

Next, we aimed to examine whether perirhinal input to L1 is crucial for memory formation in the neocortex. To specifically inhibit perirhinal axonal activity in L1 of S1 during μStim learning, we chemogenetically down-regulated synaptic transmission (14) at the axon terminals of perirhinal long-range projecting neurons without affecting their influence on other interconnected areas. We expressed hM4Di receptors (inhibitory designer receptors exclusively activated by a designer drug, DREADD (15)) in the perirhinal cortex of mice (Fig. 1D). The axon terminals in L1 of S1 were inhibited by application of exogenous ligand clozapine-N-oxide (CNO, 10 μM), injected into L1 above the stimulated region (Fig. 1D; see Methods). *Ex-vivo* experiments validated that hM4Di activation with CNO efficiently reduced light-evoked excitatory postsynaptic currents (EPSCs) (Fig. 1E). We quantified the spread of CNO in S1 by injecting the dye, Chicago Sky Blue, at the site of CNO application. Convolving perirhinal axonal density with CNO spread showed that the inhibitory action of hM4Di/CNO was predominantly in L1, where apical tuft dendrites of pyramidal neurons are located, with far less influence on the deeper layers containing the perisomatic dendrites (Fig. 1F; also see Fig. S4&S5).

Specifically blocking perirhinal cortical input to L1 of S1 severely impaired learning during the first training session (Fig. 1G&H) and resembled the effect of blocking hippocampus and/or perirhinal cortex (Fig. S2). We quantified learning as the cumulative difference between the number of successful and failed licking responses to µStim, i.e. Σ[*hits-misses*] over the whole session (see Methods). Mice for which the influence of perirhinal axons to L1 of S1 was suppressed could not learn to associate the water reward with the µStim over the first session but rather randomly licked in approximately 50% of the trials (Normalized learning score: control, 0.5±0.06, n=20 mice vs. hM4Di+/CNO+, 0.04±0.1, n=12 mice; Kruskal-Wallis test, $p<0.001$, post-hoc Dunn-Sidàk test against control, p=0.02). The effect of blocking perirhinal input to L1 (or blocking the hippocampus) also did not completely prevent transient associations between the µStim and reward and contrasted with untrained mice (i.e. mice that had never experienced a reward paired with µStim) that hardly ever responded to µStim (Fig. 1G&H; Untrained -0.5±0.05, n=5 mice, Kruskal-Wallis test, $p<0.001$, post-hoc Dunn-Sidàk test against control, $p<0.001$). CNO alone without expression of hM4Di or hM4Di expression alone without CNO application had no effect on learning (hM4Di-/CNO-, n=10 mice vs. hM4Di-/CNO+, n=7 mice vs. hM4Di+/CNO-, n=3 mice, Kruskal-Wallis test, p=0.1; Fig. S6) (16). After 3-4 sessions, the performance of control mice plateaued at improved performance levels and these animals were considered experts in the task (Expert hM4Di+/CNO-: 0.9±0.04, n=3 mice, Wilcoxon rank-sum test, p=0.009). After this point, the performance of expert mice could not be suppressed by inhibiting the perirhinal influence on S1 via CNO (Expert hM4Di+/CNO+: 0.8±0.08, Wilcoxon sign-rank test, p=1; Fig. 1H). Inhibiting perirhinal activity with lidocaine in expert rats did not affect the animal's performance (Fig. S2).

To distinguish the contribution of the perirhinal projection to L1 in S1 during µStim learning, we explored the influence of higher order somatosensory thalamic area, POm, that also projects to L1 in S1 and has also been implicated in different learning paradigms (4, 6, 17). To examine the influence of POm input in the µStim task, we expressed hM4Di receptors in POm using the Gpr26-cre transgenic mouse line (18, 19). Suppression of this projection from POm did not significantly impair the behavioral report of µStim (POm-hM4Di 0.3±0.2, n=7 mice, Wilcoxon rank-sum test, p=0.1; Fig. S6).

What information does the perirhinal cortex convey to S1 during µStim learning? We first examined the activity of deep layer neurons in the perirhinal cortex, which we previously identified as the source of projection to L1 of S1 (Fig 1A, Fig S1). We used juxtacellular single-cell recordings during learning (Fig. 2A, left; sessions 1-3). The firing rate of perirhinal neurons significantly increased during hit trials but decreased during miss trials (n=6 rats; firing rate: miss -8±11%, n=174 trials from n=28 neurons, Wilcoxon sign-rank test, p=0.01; hit 31±11%, n=287 trials from n=28 neurons, Wilcoxon sign-rank test, $p<0.001$; Fig. 2B-D). The responses in the perirhinal cortex were also marked by a significant increase in burst rate compared to baseline only during hit trials (burst rate: hit 56±22%, Wilcoxon sign-rank test. $p<0.001$, miss 14±21%, Wilcoxon sign-rank test, p=0.3), although the relative change of burst rate between miss and hit trials was not significant (burst rate miss vs. hit, Wilcoxon rank-sum test, p=0.1).

Next, we asked whether the increased activity in the perirhinal cortex modulated the response of neurons in S1 while the animal learnt to associate the μStim with reward. We performed juxtacellular recordings from L5 excitatory neurons in S1 during μStim learning (Fig. 2A, right and Fig. 2E). We reasoned that, because the μStim electrode was placed in L5, the stimulation affected L5 neurons the most. We confirmed *ex vivo* that perirhinal inputs arriving in L1 target the distal dendrites of L5 pyramidal neurons (Fig. S4). L5 pyramidal neurons responded heterogeneously during successful reports of μStim (i.e. Hits; Fig. 2E&F). A few neurons responded with a large and sustained increase in firing, while others did not respond or even decreased in firing. In still others, where the firing rate initially increased, this was often followed by inhibition compared to baseline and vice versa in some neurons that initially decreased in firing. Overall, 65% of the neurons were significantly modulated in firing relative to baseline (n=24 out of 37 cells; see Methods for classification). Suppressing perirhinal input to L1 reduced the fraction of significantly modulated neurons to only 33% (Fig. 2H&I; n=13 out of 36 cells, Chi-square test against control, p=0.007; see also Fig. S7). While there was a rich repertoire of responses to μStim, averaging over the whole population we saw no overall change in firing in response to μStim (Control baseline 2.4±0.4 Hz vs. post-stimulus 3.3±0.7 Hz, n=42 cells from 5 mice, Wilcoxon sign-rank test, p=0.7; hM4Di/CNO baseline 1.8±0.4 vs. 1.6±0.4 Hz, n = 41 cells from 5 mice, Wilcoxon sign-rank test, p=0.3; Fig. S7C).

Firing patterns of L5 pyramidal neurons are profoundly modulated by apical inputs, such that coincidence of somatic and apical dendritic inputs induces trains of high-frequency APs (bursts) (20–23). Burst firing also correlates with perceptual detection and depends on the activation of their apical dendrites that project to L1 (24) where the perirhinal inputs arrive. We therefore examined burst firing of the same populations of L5 neurons in control and hM4Di/CNO-treated mice. Learning to report μStim significantly modulated the burst rate in about half of the L5 pyramidal neurons in control mice (47%, n=18 out of 37 cells; Fig. 2G) compared to a significantly lower fraction (22%, n=8 out of 36 cells; Fig. 2J) in hM4Di/CNO-treated mice (control vs. hM4Di/CNO, Chi-square test, p=0.02). Contrary to average firing rate, we found a significant increase in average burst rate over the population of control L5 pyramidal neurons during learning (control: baseline 0.1±0.03 Hz vs. post-stimulus 0.2±0.07 Hz, Wilcoxon sign-rank test, p=0.03), which was abolished by chemogenetic suppression of perirhinal input to L1 of S1 (Fig. S7D; hM4Di/CNO: baseline 0.1±0.04 Hz vs. post-stimulus 0.1±0.03 Hz, Wilcoxon sign-rank test, p=0.8).

After 3 days, the animals became expert at reporting the μStim (i.e. behavior no longer improved and perirhinal input no longer impacted the behavioral response to μStim; Fig. 1H). Juxtacellular recordings from 273 L5 pyramidal neurons in expert animals revealed three distinct categories of firing responses to reward-associated μStim (Fig. 3A&C; see Fig. S8 for examples; see Methods for classification criteria). In 11% of cells in expert animals, we observed a significant increase in firing rate (n=30 out of 273 cells, Δ=21.7±7.5 Hz from baseline, Wilcoxon sign-rank test, $p<0.001$) briefly following μStim presentation ($L5^{ON}$ cells). The increase in firing rate in $L5^{ON}$ cells was also marked by a strong increase in burst rate (Δ=2.3±0.5 Hz from baseline, Wilcoxon sign-rank test, $p<0.001$; Fig. 3C & S8, pink). In a separate subpopulation consisting of 40% of neurons, there was a significant decrease in firing (n=108 out of 273 cells, Δ=-6.6±0.5 Hz from baseline, Wilcoxon sign-rank

test, $p<0.001$) immediately following stimulus presentation ($L5^{OFF}$ cells). Almost half of the recorded neurons (49%) showed no response to μStim (n=135 out of 273 cells, $L5^{NR}$ cells). The average baseline activity of L5 neurons in untrained rats was significantly lower than experts (Firing rate: untrained 1.2±0.1 vs. experts 4.8±0.3 Hz, Wilcoxon rank-sum test, $p<0.001$; Burst rate: untrained 0.1±0.02 Hz vs. experts 0.5±0.07 Hz, Wilcoxon rank-sum test, $p<0.001$; Fig. S9). However, the vast majority of L5 pyramidal neurons in untrained rats was non-responsive to μStim delivered at the same intensity (95% $L5^{NR}$, n=63 out of 66 cells) with a very small population positively modulated although not significantly at a population level (5% $L5^{ON}$, n=3 out of 66 cells, Δ=11.9±7.6 Hz from baseline, Wilcoxon sign-rank test, p=0.3; Fig. S9). The lack of response to μStim in untrained animals shows that the direct effect of μStim on cell firing was very modest and highlights the conclusion that the development of stereotypical and bursty firing responses in L5 pyramidal neurons is induced by learning.

The emergence of a strongly bursty subpopulation of L5 pyramidal neurons ($L5^{ON}$; Fig. 3C) following learning, suggests that learning might enhance dendritic activity, because dendritic activity causes burst firing in L5 pyramidal neurons (20, 21, 25). We therefore examined Ca^{2+}-dependent activity in the apical dendrites of L5 neurons in S1 using two-photon microscopy in expert mice. We expressed GCaMP6s in Rbp4-Cre transgenic mice (26) expressing Cre-recombinase in L5 cortical neurons and imaged at a depth of 154±2.1 μm, the region of the apical dendrite known for initiation of dendritic Ca^{2+} spikes (21) (Fig. 3D-E). Ca^{2+} transients measured from 1 s prior to, and 2 s following μStim presentation (Fig. 3F) in 318 dendrites (n=4 mice), revealed three populations with distinct fluorescence profiles (Fig. 3G). Dendritic responses closely resembled the classes of somatic responses, with 10% of dendrites showing substantial increases in fluorescence following μStim ("ON" dendrites). 37% of dendrites showed reduced Ca^{2+} fluorescence ("OFF" dendrites) and the rest were not responsive to μStim (53%, "NR" dendrites).

The emergence of three distinct populations of dendritic Ca^{2+} responses in the same proportions as the populations of somatic firing classes suggests a tight coupling of dendritic Ca^{2+} with somatic activity consistent with previous studies (20, 27–29). However, was the learning dependent on the dendritic Ca^{2+}? We tested this by activating GABAB receptors with baclofen injected locally to the superficial layers of S1 during learning (24, 30–33) (Fig. 3H, upper). This approach has previously been shown to suppress dendritic Ca^{2+} activity both *in vitro* and *in vivo* (24, 30–33; For a discussion of the limitations of this approach, see Fig. S10). Baclofen disrupted learning relative to control mice (Baclofen 0.2±0.05, n=6 mice vs. control 0.5±0.06, n=20 mice, Wilcoxon rank-sum test, p=0.01; Fig 3I-J), to an extent similar to the downregulation of perirhinal inputs to L1 described earlier (Fig. 1H). We reasoned that if dendritic activity is necessary for learning, activating the endogenous cortical circuitry responsible for direct suppression of dendritic activity should result in a similar learning deficit. We activated ChR2-expressing somatostatin-positive (SST) neurons, which suppress dendritic activity (5, 6, 8, 34, 35) during learning (Fig. 3H, lower). Activation of SST interneurons during training completely abolished the ability of mice to learn to associate μStim with water reward (SST -0.4±0.07, n=6 mice vs. control 0.5±0.06, n=20 mice, Wilcoxon rank-sum test, $p<0.001$; Fig. 3I&J). At present, there is no method to specifically block dendritic Ca^{2+} actively (for instance, SST neurons do not

exclusively target the apical dendrites of L5 pyramidal neurons (36)). Nevertheless, these manipulations, together with the observation that dendritic Ca^{2+} correlates with learning-induced changes in firing activity, suggest that a dendritic mechanism underlies the μStim learning and would also explain the importance of medial temporal input to L1 and the increased burstiness of L5 neurons.

What is the role of bursting during neocortical memory processing? Although it has long been suggested that bursting might be an important hallmark of the neural code (37, 38), and downstream mechanisms for decoding high-frequency firing are known to exist (39–41), it has never been conclusively demonstrated that bursts are a critical unit of neural information. Here, we tested the hypothesis that the firing pattern of L5 pyramidal neurons in S1 influenced the behavior of the animal in a μStim detection task (Fig. 4A). We first trained rats to respond expertly to μStim and then manipulated the firing of single L5 neurons in S1 using juxtacellular stimulation, termed “nanostimulation” (Fig. 4B). Consistent with previous studies (13, 42), rats could detect brief stimulation of a single L5 neuron (nanostimulation trials) interleaved with μStim trials (Fig. 4C-D). A previous study has shown that nanostimulation is only effective in expert rats that have learned to reliably respond to weak μStim currents and is ineffective in producing a behavioral response in naive animals (Naive, 7.5%, n=3/40 trials from n=17 cells vs. Learned, 33.5%, n=76/227 trials from n=28 cells, Chi-square test: p=0.0009; 13). The ability to detect the activity of a single neuron occurred only when the AP firing consisted of a high-frequency burst (average 106.2±7.6 Hz; n=28 cells) compared to catch trials, where no current was injected to the neuron (Burst hit rate: 31.8±4.1% vs. Catch rate: 25.6±3.5%, n=28 cells, one-sided paired t-test, p=0.02; Fig. 4C-E, top row). Stimulating the same set of neurons to fire a similar number of regular APs (average 35.1±2.4 Hz, n=28 cells) failed to induce behavioral report of nanostimulation compared to catch trials (Regular hit rate: 27.9±3.9%, n=28 cells vs. Catch rate: 25.6±3.5%, one-sided paired t-test, p=0.2; Fig. 4C-E, 2nd row). For these experiments, we made no attempt to target and stimulate a priori $L5^{ON}$ cells to elicit a behavioral report and found that behavior was also elicited by nanostimulation of ‘NR’ and/or ‘OFF’ neurons (Fig S11). One possible explanation is that $L5^{ON}$ neurons, which were defined in expert animals, established the smallest population (‘engram’) that is sufficient for behavior, but that a larger number of neurons could influence behavior under the correct circumstances, e.g. bursts. This raises the possibility that engram neurons are uniquely marked by their bursting behavior in addition to their overall firing rate. In summary, we show that burst firing increases the saliency of cortical neurons and that learning disproportionately enhances burst firing behavior.

Discussion

We found that the perirhinal projection to L1 of neocortex is crucial for learning a cortical and hippocampal dependent μStim task. This involves the emergence of distinct neuronal subpopulations marked by burst firing, correlated with an increase in their dendritic Ca^{+2} activity. We have shown previously that apical dendritic activity in L5 neurons is causally related to an (expert) rodent’s ability to detect a sensory stimulus (24, 43). Several other studies have demonstrated that dendritic activity is generated by long-range cortico-cortical input to L1 (7, 9) that is crucial for learning (34, 44, 45). The fact that perirhinal

input to neocortical L1 is also crucial for memory formation (Fig. 4F, “No Learning”) but not for sensory perception (Fig. 4F, “Expert”), suggests that perirhinal input to the apical dendrites serve as a gating signal for the enhancement of these long-range, cortico-cortical contextual inputs (Fig. 4F, “Learning”). Moreover, converging evidence implies that perceptual detection involves the reintegration of sensory-driven, feedforward and cortically-driven, contextual information arriving in the basal and apical compartments of L5 cortical pyramidal neurons respectively (7, 9, 24, 46–49). Our data therefore imply that medial-temporal-dependent learning predominantly involves the plasticity of cortically-driven, contextual information, which would have ramifications not only for our understanding of the brain but also for the principles of learning in artificial recurrent networks (50). In summary, we show that the medial temporal input to the neocortex enables memory formation via a process in L1 that likely enhances dendritic Ca^{+2} activity of distinct L5 excitatory subpopulations and promotes burst firing in these, serving as the neural signature of memory in the neocortex.

Supplementary Material

Refer to Web version on PubMed Central for supplementary material.

Acknowledgements

The authors thank Moritz von Heimendahl for preliminary discussions and analysis, Noam Nitzan for assisting in-vitro experiment, and Jaan Aru, Brett Mensh and members of the Larkum lab for helpful discussions. We thank SciDraw (Luigi Petrucco) for the rodent head schematic used in the summary figure and Fig. 4.

Funding

The research was supported by German Research Foundation (EXC 257 NeuroCure and Project number 327654276 – SFB 1315) and European Union Horizon 2020 Research and Innovation Programme (under grant agreement numbers 785907/HBP SGA2 and 670118/ERC ActiveCortex). RN is funded by Discovery grant of the Natural Sciences and Engineering Research Council of Canada (NSERC) and Project grant from the Canadian Institutes for Health Research.

Data and materials availability

All data is available from a GIN repository at the following URL: https://gin.g-node.org/larkumlab/Doron_Shin_PRhL1_paper_data. Customized MATLAB and Python codes are available upon request.

References and Notes

1. Eichenbaum H. A cortical–hippocampal system for declarative memory. Nat Rev Neurosci. 2000; 1: 41–50. [PubMed: 11252767]
2. Rolls ET. A computational theory of episodic memory formation in the hippocampus. Behav Brain Res. 2010; 215: 180–196. [PubMed: 20307583]
3. Letzkus JJ, Wolff SBE, Meyer EMM, Tovote P, Courtin J, Herry C, Lüthi A. A disinhibitory microcircuit for associative fear learning in the auditory cortex. Nature. 2011; 480: 331–335. [PubMed: 22158104]
4. Gambino F, Pagès S, Kehayas V, Baptista D, Tatti R, Carleton A, Holtmaat A. Sensory-evoked LTP driven by dendritic plateau potentials in vivo. Nature. 2014; 515: 116–119. [PubMed: 25174710]

5. Abs E, Poorthuis RB, Apelblat D, Conzelmann K-K, Spiegel I, Letzkus JJ. Learning-Related Plasticity in Dendrite-Targeting Layer 1 Interneurons. Neuron. 2018; 100: 684–699. [PubMed: 30269988]
6. Williams LE, Holtmaat A. Higher-Order Thalamocortical Inputs Gate Synaptic Long-Term Potentiation via Disinhibition. Neuron. 2019; 101: 91–102. [PubMed: 30472077]
7. Xu NL, Harnett MT, Williams SR, Huber D, O'Connor DH, Svoboda K, Magee JC. Nonlinear dendritic integration of sensory and motor input during an active sensing task. Nature. 2012; 492: 247–251. [PubMed: 23143335]
8. Cichon J, Gan W-B. Branch-specific dendritic Ca^{2+} spikes cause persistent synaptic plasticity. Nature. 2015; 520: 180–185. [PubMed: 25822789]
9. Manita S, Matsumoto T, Nakai J, Yanagawa Y, Odagawa M, Suzuki T, Larkum ME, Ohkura M, Yamanaka A, Ota K, Sato M, et al. A Top-Down Cortical Circuit for Accurate Sensory Perception. Neuron. 2015; 86: 1304–1316. [PubMed: 26004915]
10. Witter MP, Groenewegen HJ. Connections of the parahippocampal cortex in the cat. III. Cortical and thalamic efferents. J Comp Neurol. 1986; 252: 1–31. [PubMed: 3793972]
11. Agster KL, Burwell RD. Cortical efferents of the perirhinal, postrhinal, and entorhinal cortices of the rat. Hippocampus. 2009; 19: 1159–1186. [PubMed: 19360714]
12. Squire LR, Stark CEL, Clark RE. THE MEDIAL TEMPORAL LOBE. Annu Rev Neurosci. 2004; 27: 279–306. [PubMed: 15217334]
13. Houweling AR, Brecht M. Behavioural report of single neuron stimulation in somatosensory cortex. Nature. 2008; 451: 65–68. [PubMed: 18094684]
14. Stachniak TJ, Ghosh A, Sternson SM. Chemogenetic Synaptic Silencing of Neural Circuits Localizes a Hypothalamus→Midbrain Pathway for Feeding Behavior. Neuron. 2014; 82: 797–808. [PubMed: 24768300]
15. Armbruster BN, Li X, Pausch MH, Herlitze S, Roth BL. Evolving the lock to fit the key to create a family of G protein-coupled receptors potently activated by an inert ligand. Proc Natl Acad Sci U S A. 2007; 104: 5163–8. [PubMed: 17360345]
16. Gomez JL, Bonaventura J, Lesniak W, Mathews WB, Sysa-Shah P, Rodriguez LA, Ellis RJ, Richie CT, Harvey BK, Dannals RF, Pomper MG, et al. Chemogenetics revealed: DREADD occupancy and activation via converted clozapine. Science. 2017; 357 doi: 10.1126/science.aan2475
17. Audette NJ, Bernhard SM, Ray A, Stewart LT, Barth AL. Rapid Plasticity of Higher-Order Thalamocortical Inputs during Sensory Learning. Neuron. 2019; 103: 277–291. [PubMed: 31151774]
18. Oram TB, Ahissar E, Yizhar O. Soc Neuro Abstr.
19. Zolnik TA, Ledderose J, Toumazou M, Trimbuch T, Oram T, Rosenmund C, Eickholt BJ, Sachdev RNS, Larkum ME. Layer 6b Is Driven by Intracortical Long-Range Projection Neurons. Cell Rep. 2020; 30: 3492–3505. [PubMed: 32160552]
20. Larkum ME, Zhu JJ, Sakmann B. A new cellular mechanism for coupling inputs arriving at different cortical layers. Nature. 1999; 398: 338–341. [PubMed: 10192334]
21. Larkum ME, Zhu JJ. Signaling of layer 1 and whisker-evoked Ca^{2+} and Na^{+} action potentials in distal and terminal dendrites of rat neocortical pyramidal neurons in vitro and in vivo. J Neurosci. 2002; 22: 6991–7005. [PubMed: 12177197]
22. Schwindt P, Crill W. Mechanisms Underlying Burst and Regular Spiking Evoked by Dendritic Depolarization in Layer 5 Cortical Pyramidal Neurons. J Neurophysiol. 1999; 81: 1341–1354. [PubMed: 10085360]
23. Larkum ME, Senn W, Lüscher HR. Top-down dendritic input increases the gain of layer 5 pyramidal neurons. Cereb Cortex. 2004; 14: 1059–1070. [PubMed: 15115747]
24. Takahashi N, Oertner TG, Hegemann P, Larkum ME. Active cortical dendrites modulate perception. Science. 2016; 354: 1587–1590. [PubMed: 28008068]
25. Williams SR, Stuart GJ. Mechanisms and consequences of action potential burst firing in rat neocortical pyramidal neurons. J Physiol. 1999; 521: 467–482. [PubMed: 10581316]
26. Gerfen CR, Paletzki R, Heintz N. GENSAT BAC Cre-Recombinase Driver Lines to Study the Functional Organization of Cerebral Cortical and Basal Ganglia Circuits. Neuron. 2013; 80: 1368–1383. [PubMed: 24360541]

27. Helmchen F, Svoboda K, Denk W, Tank DW. In vivo dendritic calcium dynamics in deep-layer cortical pyramidal neurons. Nat Neurosci. 1999; 2: 989–996. [PubMed: 10526338]
28. Beaulieu-Laroche L, Toloza EHS, Brown NJ, Harnett MT. Widespread and Highly Correlated Somato-dendritic Activity in Cortical Layer 5 Neurons. Neuron. 2019; 103: 235–241. [PubMed: 31178115]
29. Francioni V, Padamsey Z, Rochefort NL. High and asymmetric somato-dendritic coupling of V1 layer 5 neurons independent of visual stimulation and locomotion. Elife. 2019; 8 doi: 10.7554/eLife.49145
30. Pérez-Garci E, Gassmann M, Bettler B, Larkum ME. The $GABA_{B1b}$ Isoform Mediates Long-Lasting Inhibition of Dendritic Ca^{2+} Spikes in Layer 5 Somatosensory Pyramidal Neurons. Neuron. 2006; 50: 603–616. [PubMed: 16701210]
31. Pérez-Garci E, Larkum ME, Nevian T. Inhibition of dendritic Ca^{2+} spikes by GABAB receptors in cortical pyramidal neurons is mediated by a direct Gi/o-βγ-subunit interaction with Cav1 channels. J Physiol. 2013; 591: 1599–1612. [PubMed: 23184512]
32. Palmer LM, Schulz JM, Murphy SC, Ledergerber D, Murayama M, Larkum ME. The Cellular Basis of GABAB-Mediated Interhemispheric Inhibition. Science. 2012; 335: 989–993. [PubMed: 22363012]
33. Suzuki M, Larkum ME. Dendritic calcium spikes are clearly detectable at the cortical surface. Nat Commun. 2017; 8 276 [PubMed: 28819259]
34. Makino H, Komiyama T. Learning enhances the relative impact of top-down processing in the visual cortex. Nat Neurosci. 2015; 18: 1116–1122. [PubMed: 26167904]
35. Chen SX, Kim AN, Peters AJ, Komiyama T. Subtype-specific plasticity of inhibitory circuits in motor cortex during motor learning. Nat Neurosci. 2015; 18: 1109–1115. [PubMed: 26098758]
36. Wang Y, Toledo-Rodriguez M, Gupta A, Wu C, Silberberg G, Luo J, Markram H. Anatomical, physiological and molecular properties of Martinotti cells in the somatosensory cortex of the juvenile rat. J Physiol. 2004; 561: 65–90. [PubMed: 15331670]
37. Crick F. Function of the thalamic reticular complex: The searchlight hypothesis. Proc Natl Acad Sci U S A. 1984; 81: 4586–4590. [PubMed: 6589612]
38. Lisman JE. Bursts as a unit of neural information: Making unreliable synapses reliable. Trends Neurosci. 1997; 20: 38–43. [PubMed: 9004418]
39. Markram H, Wang Y, Tsodyks M. Differential signaling via the same axon of neocortical pyramidal neurons. Proc Natl Acad Sci U S A. 1998; 95: 5323–5328. [PubMed: 9560274]
40. Izhikevich EM, Desai NS, Walcott EC, Hoppensteadt FC. Bursts as a unit of neural information: Selective communication via resonance. Trends Neurosci. 2003; 26: 161–167. [PubMed: 12591219]
41. Naud R, Sprekeler H. Sparse bursts optimize information transmission in a multiplexed neural code. Proc Natl Acad Sci. 2018; 115: E6329–E6338. [PubMed: 29934400]
42. Doron G, von Heimendahl M, Schlattmann P, Houweling AR, Brecht M. Spiking Irregularity and Frequency Modulate the Behavioral Report of Single-Neuron Stimulation. Neuron. 2014; 81: 653–663. [PubMed: 24507196]
43. Takahashi N, Ebner C, Sigl-Glöckner J, Moberg S, Nierwetberg S, Larkum ME. Active dendritic currents gate descending cortical outputs in perception. Nat Neurosci. 2020; 2020: 1–9.
44. Miyamoto D, Hirai D, Fung CCA, Inutsuka A, Odagawa M, Suzuki T, Boehringer R, Adaikkan C, Matsubara C, Matsuki N, Fukai T, et al. Top-down cortical input during NREM sleep consolidates perceptual memory. Science. 2016; 352: 1315–1318. [PubMed: 27229145]
45. Payeur A, Guerguiev J, Zenke F, Richards B, Naud R. bioRxiv Neurosci. doi: 10.1101/2020.03.30.015511
46. Larkum M. A cellular mechanism for cortical associations: An organizing principle for the cerebral cortex. Trends Neurosci. 2013; 36: 141–151. [PubMed: 23273272]
47. Felleman DJ, Van Essen DC. Distributed Hierarchical Processing in the Primate Cerebral Cortex. Cereb Cortex. 1991; 1: 1–47. [PubMed: 1822724]
48. Ranganathan GN, Apostolides PF, Harnett MT, Xu N-L, Druckmann S, Magee JC. Active dendritic integration and mixed neocortical network representations during an adaptive sensing behavior. Nat Neurosci. 2018; doi: 10.1038/s41593-018-0254-6

49. Suzuki M, Larkum ME. General Anesthesia Decouples Cortical Pyramidal Neurons. Cell. 2020; 180: 666–676. [PubMed: 32084339]
50. Kreiman G, Serre T. Beyond the feedforward sweep: feedback computations in the visual cortex. Ann N Y Acad Sci. 2020; 1464: 222–241. [PubMed: 32112444]
51. Madisen L, Mao T, Koch H, Zhuo J, Berenyi A, Fujisawa S, Hsu Y-WA, Garcia AJ, Gu X, Zanella S, Kidney J, et al. A toolbox of Cre-dependent optogenetic transgenic mice for light-induced activation and silencing. Nat Neurosci. 2012; 15: 793–802. [PubMed: 22446880]
52. Lefort S, Tomm C, Floyd Sarria JC, Petersen CCH. The Excitatory Neuronal Network of the C2 Barrel Column in Mouse Primary Somatosensory Cortex. Neuron. 2009; 61: 301–316. [PubMed: 19186171]
53. Franklin, K, Paxinos, G. The Mouse Brain in Stereotaxic Coordinates. Academic Press; San Diego: 2001.
54. Paxinos, G, Watson, C. The Rat Brain in Stereotaxic Coordinates. Academic Press; San Diego: 1998.
55. Lüscher C, Jan LY, Stoffel M, Malenka RC, Nicoll RA. G protein-coupled inwardly rectifying K^+ channels (GIRKs) mediate postsynaptic but not presynaptic transmitter actions in hippocampal neurons. Neuron. 1997; 19: 687–695. [PubMed: 9331358]
56. Sanchez-Vives MV, Barbero-Castillo A, Perez-Zabalza M, Reig R. GABAB receptors modulation of thalamocortical dynamics and synaptic plasticity. Neuroscience. 2020; doi: 10.1016/j.neuroscience.2020.03.011

One Sentence Summary

Perirhinal cortex gates memory formation in neocortical layer 1

Europe PMC Funders Author Manuscripts

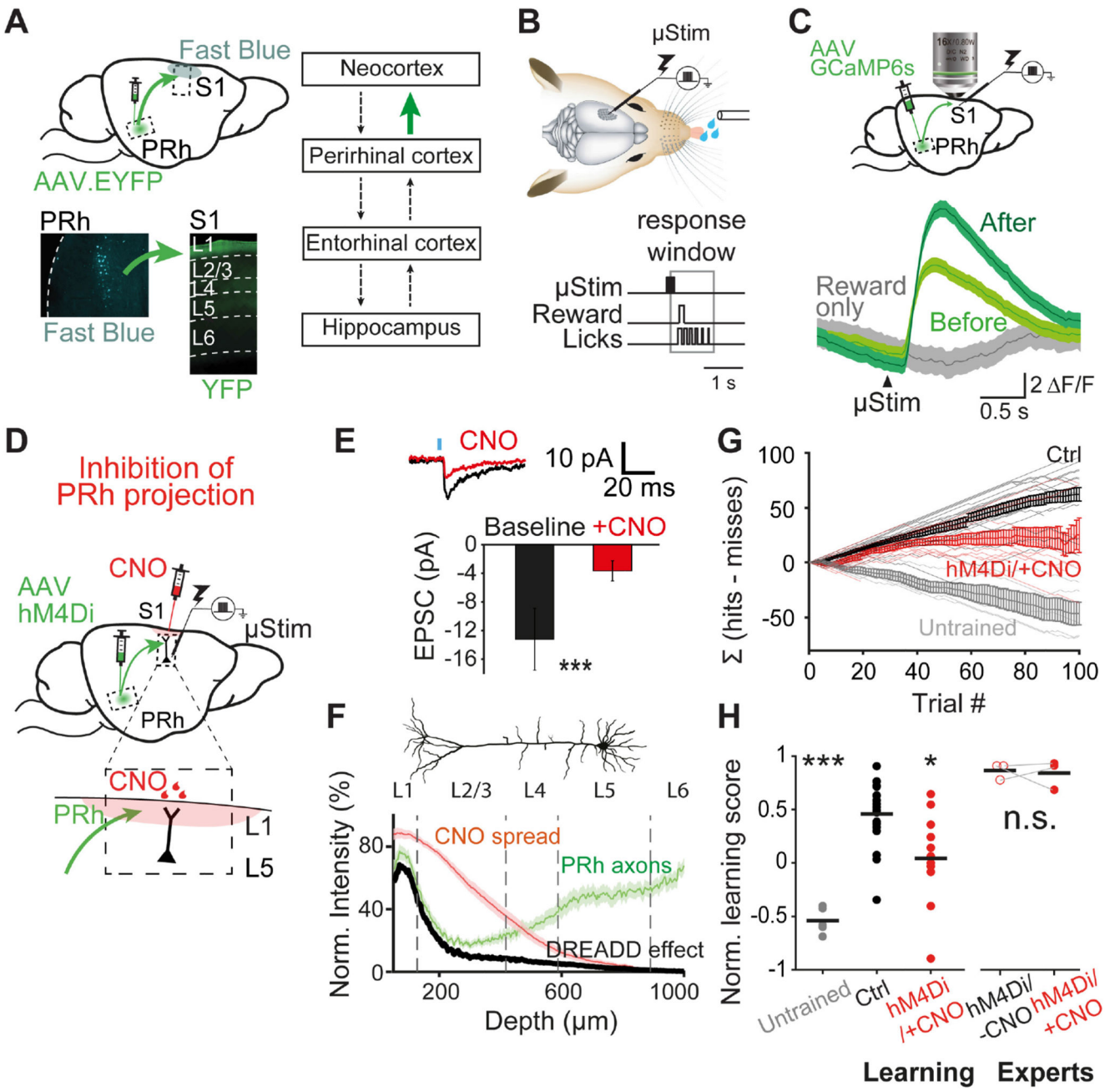

Fig. 1. Hippocampus via perirhinal cortex projects to neocortical L1 and is necessary forlearning a µStim task.

(A) Perirhinal (PRh) projection to S1. Lower left, retrograde tracing. PRh deep layer neurons were labeled with Fast Blue after application to L1 of S1. Lower right, anterograde tracing. ChR2/EYFP labeled axons of PRh project to L1 of S1. Right, simplified connectivity map between the neocortex, perirhinal cortex, entorhinal cortex and hippocampus (12). Investigated connection in green. **(B)** Upper, schematic of µStim detection task. Tungsten electrode was placed in L5 of S1. Lower, animals were trained to lick within a 1.1-s window following µStim. **(C)** Upper, schematic of two-photon axonal imaging of

GCaMP6s-expressing PRh axons in L1 of S1. Lower, Ca^{2+} transients of PRh axons in response to μStim before and after the first μStim training session. **(D)** Schematic of chemogenetic silencing of PRh axons in L1 of S1 during μStim task. AAV.hM4Di was injected to PRh and CNO was applied locally to L1 of S1 before starting the training session. Inset, enlarged view of CNO injection site in S1. **(E)** Chemogenetic suppression of synaptic transmission *ex vivo*. Average EPSC amplitudes at the cell body of L5 pyramidal neurons following blue light on L1 before and after CNO application. Wilcoxon sign-rank test. ***p<0.001, n=13 cells. **(F)** Spatial profile of DREADD effect estimated by the spread of dye and the fluorescence intensity of PRh/YFP axons as a function of cortical depth. **(G)** Cumulative difference between the numbers of hit and miss trials (Σ [*hits-misses*]) in the first training session. Light lines represent individual mice and bold lines represent the mean and SEM. **(H)** Normalized learning score of untrained (n=5), control (n=20) and mice under PRh axonal suppression during learning (hM4Di/+CNO, n=12). Kruskal-walis test, p<0.001, post-hoc Dunn-Sidàk test against control, *p<0.05, ***p<0.001. CNO did not affect the learning score of expert mice expressing hM4Di receptors in PRh (experts). Wilcoxon sign-rank test, n.s., p=1. Each dot corresponds to individual mice and black line represents mean.

Europe PMC Funders Author Manuscripts

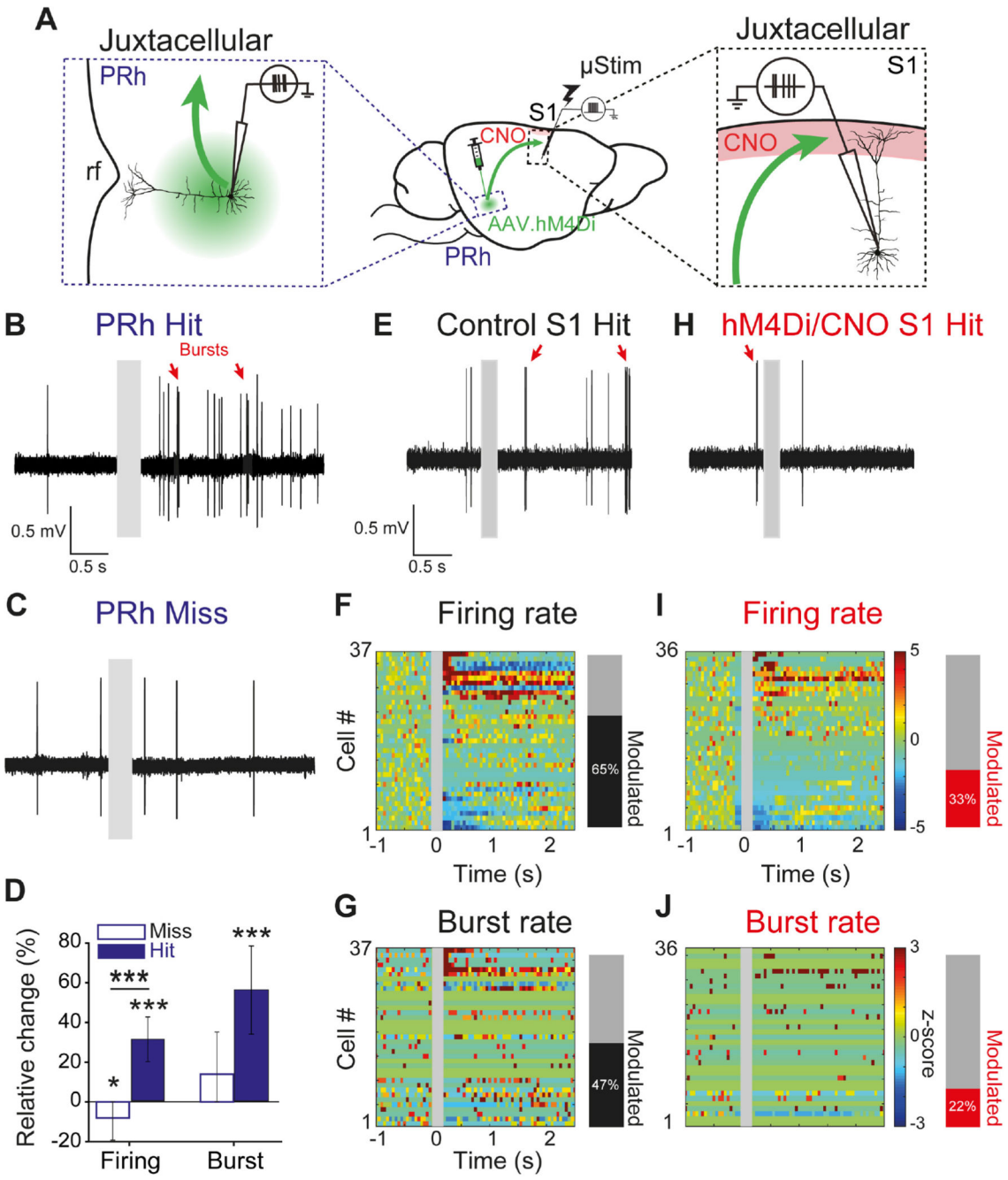

Fig. 2. Enhanced perirhinal activity in hit trials modulates neocortical activity during learning.

(A) Experimental paradigm: single-cell, juxtacellular recordings from deep layer pyramidal neurons in PRh (left) and L5 pyramidal neurons in S1 (right). Red: CNO injection site in L1 of S1, rf: rhinal fissure. **(B), (C)** High-pass filtered recording traces from an example PRh neuron during a hit and a miss trial, respectively. Gray box: period of μStim. (**D)** Relative changes in firing rate and burst rate during miss and hit trials from PRh neurons. *p<0.05, ***p<0.001. **(E), (H)** High-pass filtered recordings from an example neuron in S1 during a hit trial in control and hM4Di/CNO mice, respectively. Gray box: period of μStim. Red

arrows: bursts. **(F), (I)** Left, heat map of z-score for normalized firing rates of individual L5 neurons in S1 of control and hM4Di/CNO mice, respectively. Z-scores for cells with no spikes during the pre-stimulus period could not be computed and were therefore not included in this analysis. Right, fraction of significantly modulated neurons in control and hM4Di/CNO S1, respectively (see Methods for classification criteria). **(G), (J)** Same as **(F)** and **(I)** but burst rate for the same cells. Cell number is constant and cells with no burst events during pre-stimulus period are marked with zeros (green).

Europe PMC Funders Author Manuscripts

Europe PMC Funders Author Manuscripts

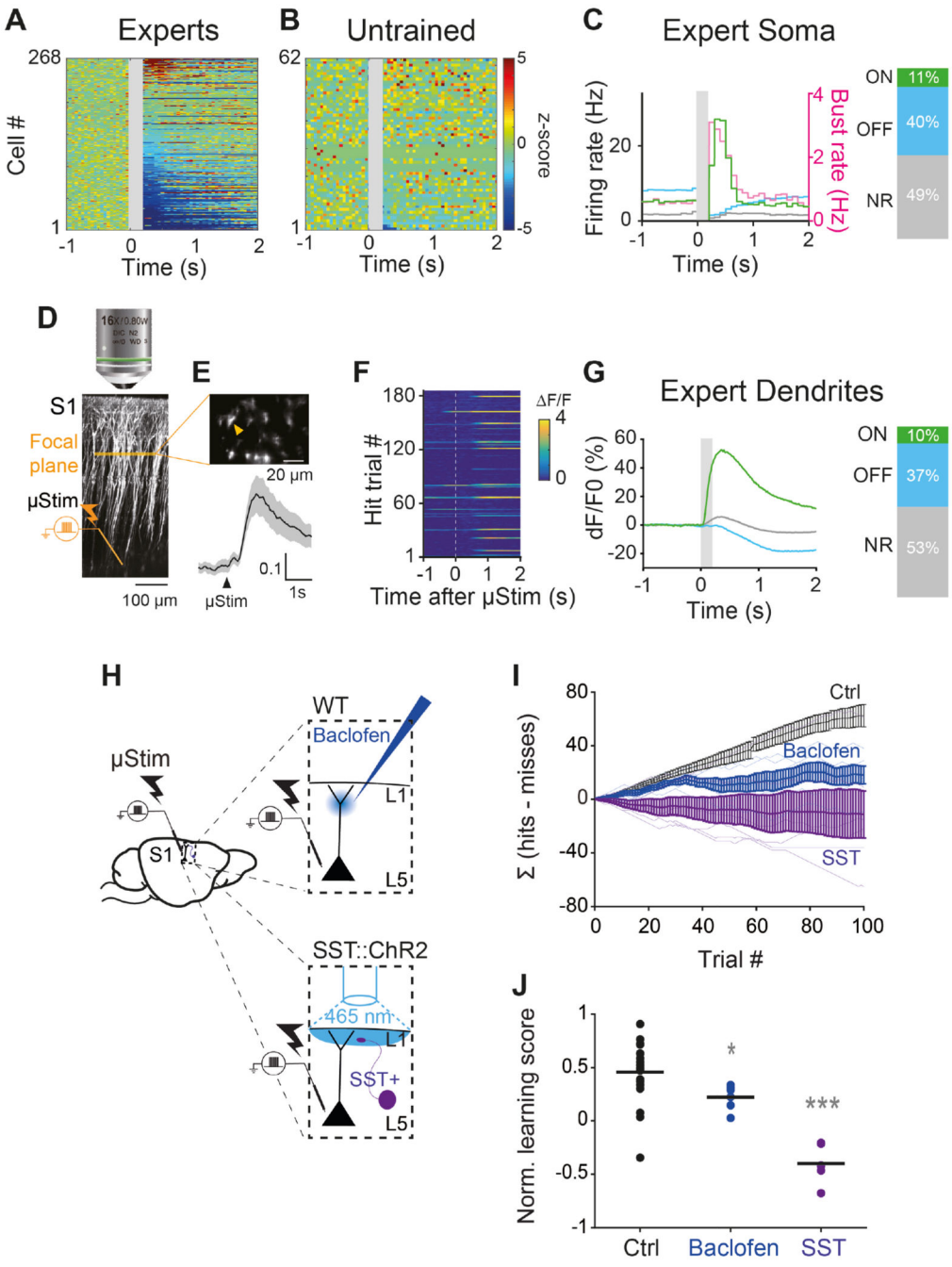

Fig. 3. Emergence of distinct populations following learning depends on apical dendritic activity of L5 pyramidal neurons.

(A), **(B)** Z-score normalized firing rate PSTHs of L5 pyramidal neurons in S1 of expert and untrained rats, respectively. Z-scores for cells with no spikes during pre-stimulus period could not be computed and therefore not included in this analysis. **(C)** Left, average PSTHs of $L5^{ON}$, $L5^{OFF}$ and $L5^{NR}$ neurons (total n=273 cells) in expert rats. Gray box: µStim. Right, the fraction of $L5^{ON}$, $L5^{OFF}$ and $L5^{NR}$ neurons. **(D)** Two-photon Ca^{2+} imaging from the apical dendrites of L5 pyramidal neurons in Rbp4-cre transgenic mice during the

μStim task. **(E)** Horizontal imaging plane (upper) (~150 μm from pia) and average Ca^{2+} responses (lower) for all trials from an example dendrite marked with a yellow arrow. **(F)** Ca^{2+} responses in an apical dendrite marked in **(E)** during 180 trials of hit trials. **(G)** Left, Average peri-stimulus Ca^{2+} responses in ON, OFF and NR dendrites (total n=318 dendrites) during hit trials. Gray box: μStim. Right, fraction of ON, OFF and NS dendrites. **(H)** Experimental designs for manipulating dendritic activity during μStim task. Upper, baclofen application in superficial layers of S1 in wild-type mice. Lower, optogenetic activation of SST+ interneurons during μStim task in SST::ChR2 transgenic mice. The surface of the craniotomy was illuminated with blue light (465 nm) (See Methods). **(I)** Cumulative learning curve of control mice (n=20, black), baclofen-treated mice (n=6, blue) and SST::ChR2 mice (n=6, purple) during the first session. **(J)** Normalized learning score of control, baclofen-treated and SST::ChR2 mice at the first session. Each dot corresponds to individual mice and black line indicates mean. Wilcoxon rank-sum test against control, *** $p<0.001$, *$p=0.01$.

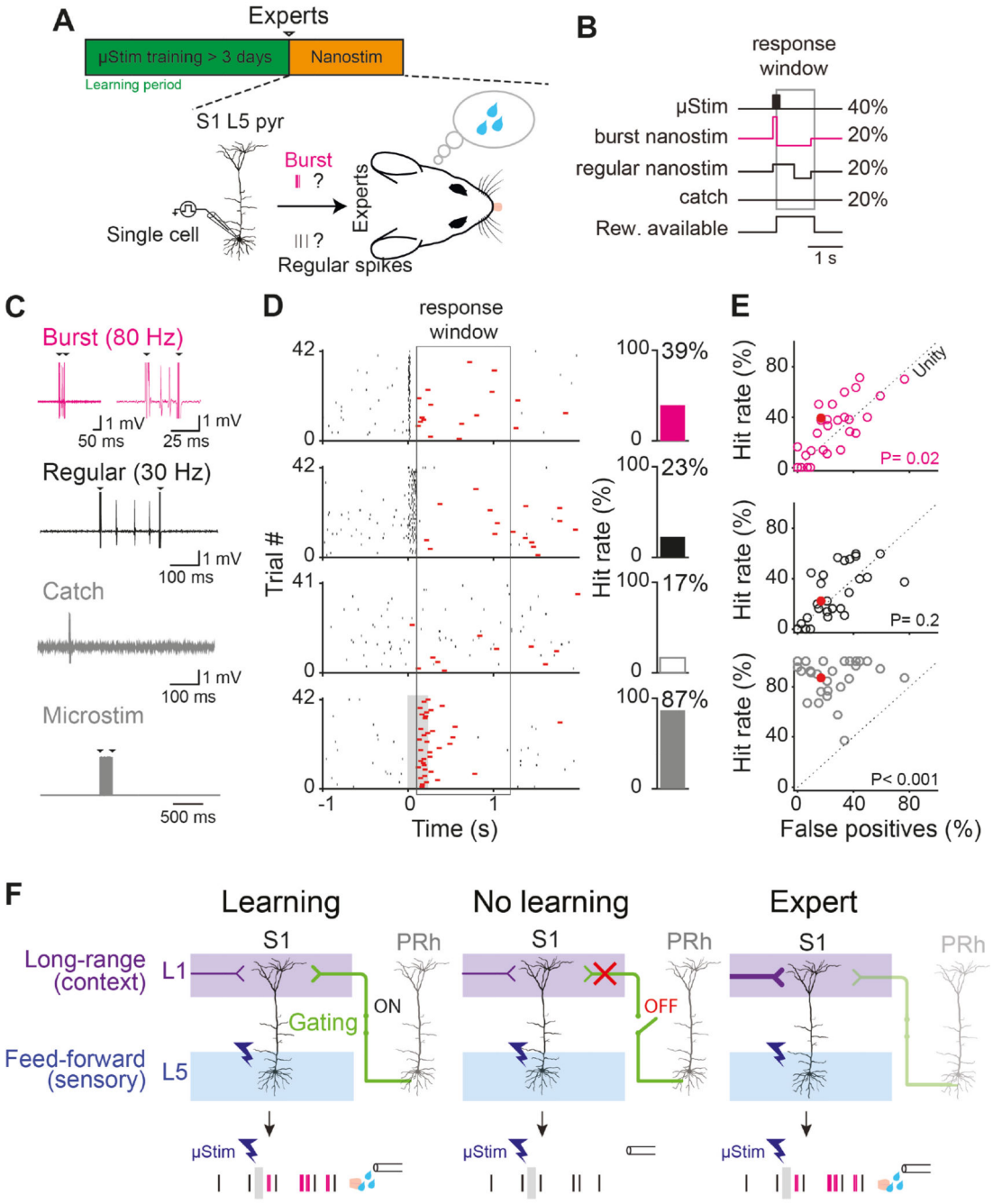

Fig. 4. Burst firing in single L5 pyramidal neurons is more salient than regular firing after learning.

(A) Experimental paradigm single-cell “nano”stimulation. Upper: Single-cell stimulation was performed after >3 days of µStim training (i.e. in expert animals). Lower, hypothesis. Do burst or regular firing differentially induce learned behavior (i.e. licking to µStim)? **(B)** Four types of stimulations were randomly presented: 40% of µStim trials, 20% of burst (80-120 Hz, pink) nanostimulation trials, 20% regular nanostimulation trials and 20% ‘catch’ trials with no current injection. **(C)** Examples of juxtacellular responses recorded

Europe PMC Funders Author Manuscripts

simultaneously during the four types of stimulations. Arrows indicate stimulation artifacts. **(D)** Left, all trials showing the spiking (black) and behavioral (red) responses to the four types of stimulation for one example L5 pyramidal neuron. Black ticks indicate spikes and red ticks indicate licking. Gray box: μStim. Right, proportion of trials with hits. **(E)** Hit rate as a function of false-positive (catch) trials (n=28 cells). Red circles indicate the example cell shown in **(D)**. Statistical significance was tested by one-sided paired t-test. Dotted line indicates the unity line. **(F)** Gating theory of memory formation in the neocortex. PRh inputs to L1 gate long-range inputs that modulate the firing mode of L5 pyramidal neurons in S1 and learning. Top row, three behavioral conditions. Bottom row, stylized representative L5 pyramidal responses.

Europe PMC Funders Author Manuscripts